Electronic Supplementary Material (ESI) for Journal of Materials Chemistry A.

Supplementary Information

Construction of Atomically Dispersed Cu Sites and S Vacancies on CdS for Enhanced Photocatalytic CO_2 Reduction

Heng Cao[‡a], Jiawei Xue[‡a], Zhiyu Wang[a], Jingjing Dong[a], Wenjie Li[a], Ruyang Wang[a], Song Sun[b], Chen Gao[c], Yisheng Tan[d], Xiaodi Zhu[a], Jun Bao*[a]*

[a] National Synchrotron Radiation Laboratory, University of Science and Technology of China, Hefei, Anhui 230029, China.

[b] School of Chemistry and Chemical Engineering, Anhui University, Hefei, Anhui, 230601, China.

[c] School of Physical Sciences, University of Chinese Academy of Sciences, Beijing, 100049, China.

[d] State Key Laboratory of Coal Conversion, Institute of Coal Chemistry, Chinese Academy of Sciences, Taiyuan 030001, China.

‡ Heng Cao and Jiawei Xue contributed equally to this work.

*Corresponding authors. E-mail: zhuxiaodi@ustc.edu.cn; baoj@ustc.edu.cn.

Experimental section.

Synthesis of CdS: The CdS nanorods were fabricated by a hydrothermal method. The FTO-coated glasses (1 × 3 cm) were cleaned by etching in 0.01 M HCl for 30 seconds and thorough rinsing in deionized water. Four pieces of cleaned FTO glasses substrates were placed vertically in a 100 mL Teflon-lined stainless-steel autoclave with the conductive sides facing down. Typically, 370 mg cadmium nitrate tetrahydrate, 274 mg thiourea and 50 mg glutathione (reduced form) were dissolved in 50 mL deionized water as the precursor solution, then it was transferred to the autoclave after stirring for 5 min. The oven was preheated to 200 °C and kept for 4 h. After the autoclave was naturally cooled down to the ambient temperature, the CdS nanorods-coated FTO glasses were obtained and washed gently by deionized water.

***Synthesis of CuCdS-m via Cation Exchange Reaction*:** The precursor solution for the cation exchange reaction was prepared in a 100 mL 3-neck flask with 28 mL of 1 M HCl. The pH was adjusted to 7 by dropwise addition of hydrazine (85%) and an additional 60 mL of deionized water was added. The solution was purged of oxygen by bubbling argon gas throughout the reaction. After a 5 min purge at room temperature, the flask was heated to 90 °C by a water bath. At 50 °C, 5 mg of copper(I) chloride was quickly added to the solution, and then the 3-neck flask was resealed immediately. After the temperature stabilized at 90 °C, the as-prepared CdS samples were dipped into the solution for 2s, 5s and 10s followed by rinsing in deionized water to form the CuCdS-m (m=2, 5, 10) samples, respectively. The as-obtained samples were calcined in argon at 400°C for an hour and followed by reduced in 10% H_2 for an hour.

***Materials characterization*:** The morphology was analyzed by a field emission SEM (Sirion200). High-resolution transmission electron microscopy (HRTEM) imaging was carried out on a FEI Talos F200X microscope operated at 200 kV. Elemental analysis of samples was conducted by inductively coupled plasma atomic emission spectrometry (Optima 7300 DV). The X-ray diffraction (XRD) patterns of samples were obtained using a Rigaku Miniflex-600 with a Cu Kα radiation (λ=0.15406 nm) at a step width of 2° min^{-1}. Electron paramagnetic resonance (EPR) spectra were obtained using a JES-FA200 (JEOL) EPR Spectrometer. The surface electronic states of samples were analyzed via X-ray photoelectron spectroscopy (XPS) with Al Kα (hv=1486.6 eV) as the excitation source (Thermo Scientific ESCALAB 250), and all binding energies were referenced to the C 1s peak at 284.6 eV of the surface adventitious carbon. The X-ray absorption fine structure (XAFS) data at Cu K-edge were recorded in fluorescence mode at 1W1B station in Beijing Synchrotron Radiation Facility (BSRF, Beijing). The acquired EXAFS data was processed according to the standard procedures using the ATHENA module implemented in the IFEFFIT software packages. Synchrotron-radiation vacuum ultraviolet photoionization mass spectrometry (SVUV-PIMS) was performed at the Combustion Endstation in the BL03U beamline of the National

Synchrotron Radiation Laboratory (NSRL, Hefei). UV–vis diffuse reflectance spectra (UV–vis DRS) were obtained using a Shimadzu UV-3700 recording spectrophotometer.

***Measurement of photocatalytic activity*:** The photocatalytic performance was evaluated in a 750 mL sealed glass reactor system at ambient temperature and atmospheric pressure. Typically, 4 pieces of as-obtained samples were placed adjacently at the bottom of the container. The system was vacuum-treated to remove the air after 1.2 mL deionized water was injected into the reactor, which was followed by filling CO_2 to the system until achieved atmospheric pressure. After a 30 min adsorption-desorption equilibrium, the system was irradiated by a 300W Xe lamp. During the irradiation, 1 mL gas was taken from the reactor at regular intervals (1 h) via a syringe and analyzed by a gas chromatograph (Agilent, GC 8860) equipped with a thermal conductivity detector (TCD), a flame ionized detector (FID) and methanizer. The sample gases were calibrated with a standard gas mixture and determined through the retention time.

***Electrochemical measurements*:** Electrochemical measurements were carried out on an electrochemical workstation (CHI660E Instruments, China) with a standard three-electrode system, whereas Ag/AgCl (saturated KCl) and a Pt wire were utilized as the reference and counter electrode, respectively. The sample was used as the working electrode and 0.5 M Na_2SO_4 electrolyte (pH=5.64) was selected as the carrier for ion transport in our electrochemical impedance spectroscopy (EIS) tests. Before our test, the electrolyte was purged with N_2 for 30 min to exclude the dissolved oxygen. Here, a −0.05 V applied bias voltage (versus RHE) was chosen for the EIS tests. The Mott-Schottky
(MS) curves were collected in dark at 1000 Hz with a scan rate of 20 mV in the mixed solution of 0.25 M Na_2S and 0.35 M Na_2SO_3.

In situ DRIFTS measurement: *In situ* diffuse reflectance infrared Fourier transform spectra (DRIFTS) tests were performed using a Nicolet iS50 FT-IR spectrometer (Thermo Fisher, USA) equipped with a liquid nitrogen cooled HgCdTe (MCT) detector. The *in situ* DRIFTS spectra were recorded by collecting 32 scans at a resolution of 8 cm^{-1}. Before the measurement, each sample was purged with He (30 mL/min) for 30 min to blow out all the gases in the cell and the adsorbed species on the samples. After that, the sample was exposed to the mixture of CO_2 (15 mL/min) and He (30 mL/min) bubbled H_2O vapor for about 30 min, the spectra were recorded in dark.

DFT computational details: The calculations were carried out using the DMol3 code and the Cambridge Sequential Total Energy Package (CASTEP) code.[1,2] Nonlocal exchange and correlation energies were treated with the Perdew−Burke−Ernzerhof functional, which was based on the generalized gradient approximation (GGA). Considering CdS (110) surface is a stable and nonpolar surface with a smaller surface energy, a 2 × 2 (110) slab (6 layers) containing 24 Cd and 24 S atoms was built. The vacuum space was set to 15 Å, which was enough to avoid the interactions between

periodic images. The van der Waals correction was employed by Grimme method in DFT-D to describe the interactions between dissociative adsorption intermediates and catalysts.[3] The double numerical plus polarization (DNP) basis set was used due to its high accuracy.[4] The convergence criterion for the energy, maximum force and maximum displacement were set at 2.0 × 10^{-5} hartree (Ha), 4.0 × 10^{-3} Ha $Å^{-1}$ and 5.0 × 10^{-3} Å, respectively. The Brillouin zone was sampled by a 2 × 2 × 1 Monkhorst−Pack k-point grid. A thermal smearing value of 0.005 Ha was used. A complete linear synchronous transit (LST) and quadratic synchronous transit (QST) search algorithm were used to determine the transition state of the reaction.[5] The CASTEP was used to calculate the band structure, density of states and electron density difference, where the convergence criteria for the energy, maximum force, maximum displacement and energy cutoff equal were set at 2.0 × 10^{-5} eV per atom, 0.05 eV $Å^{-1}$, 2.0 × 10^{-3} Å and 380 eV. The k-points were set as 2 × 2 × 1. Spin-polarized DFT + U theory is applied to correct the well-known DFT self-interaction errors for the strongly correlated electrons in the transition metal ions. Here, we use U – J (Ueff) = 2.0 eV for Cd atoms.[6]

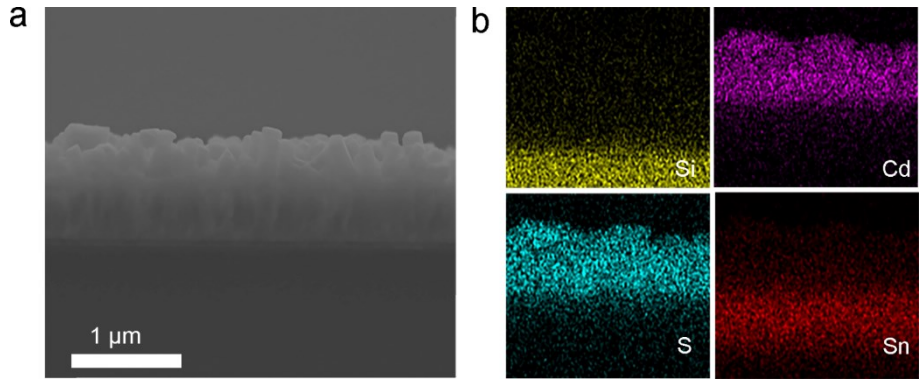

Fig. S1 SEM cross-section view image (a)and the EDS mapping images (b) of CdS.

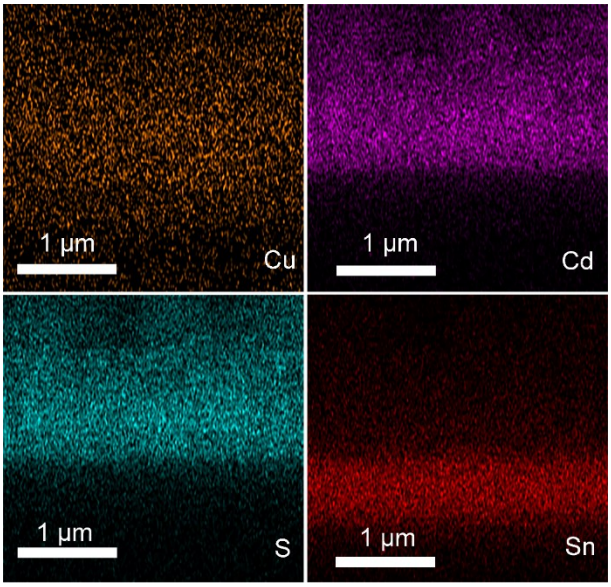

Fig. S2 The EDS mapping images of cross section view of CuCdS-5.

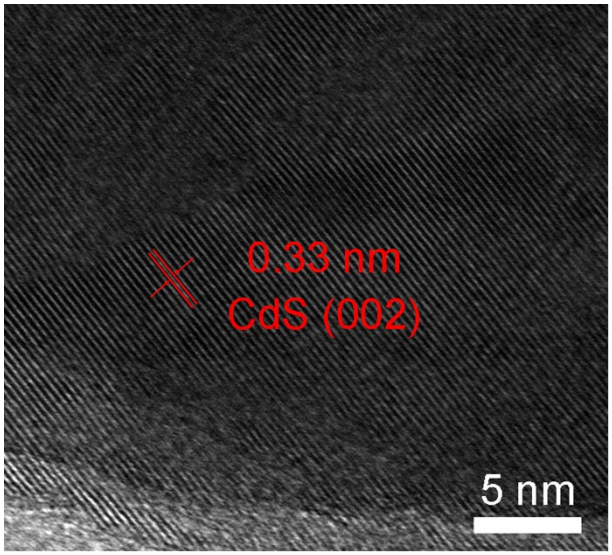

Fig. S3 HRTEM image of CuCdS-5.

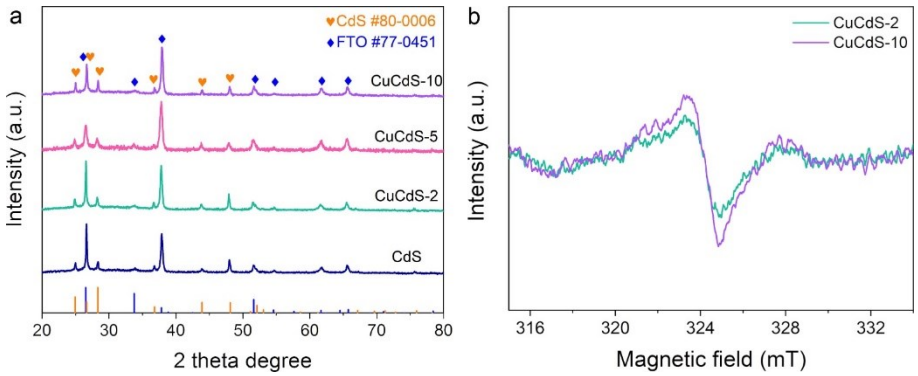

Fig. S4 XRD patterns (a) of CdS, CuCdS-2, CuCdS-5 and CuCdS-10; EPR spectra (b) of CuCdS-2 and CuCdS-10.

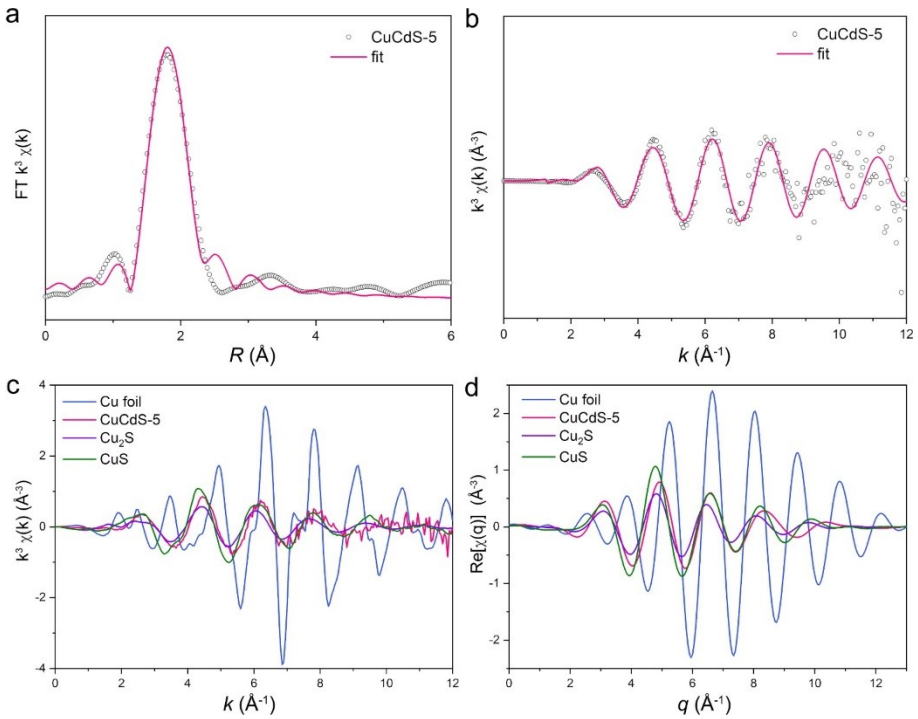

Fig. S5 (a) Fourier transformed k^3-weighted χ(k)-function of the Cu *K*-edge EXAFS spectra; (b) EXAFS spectra of the CuCdS-5 transformed in *k* space. EXAFS spectra of CuCdS-5, CdS, Cu_2S and Cu foil in *k* space (c) and *q* space (d).

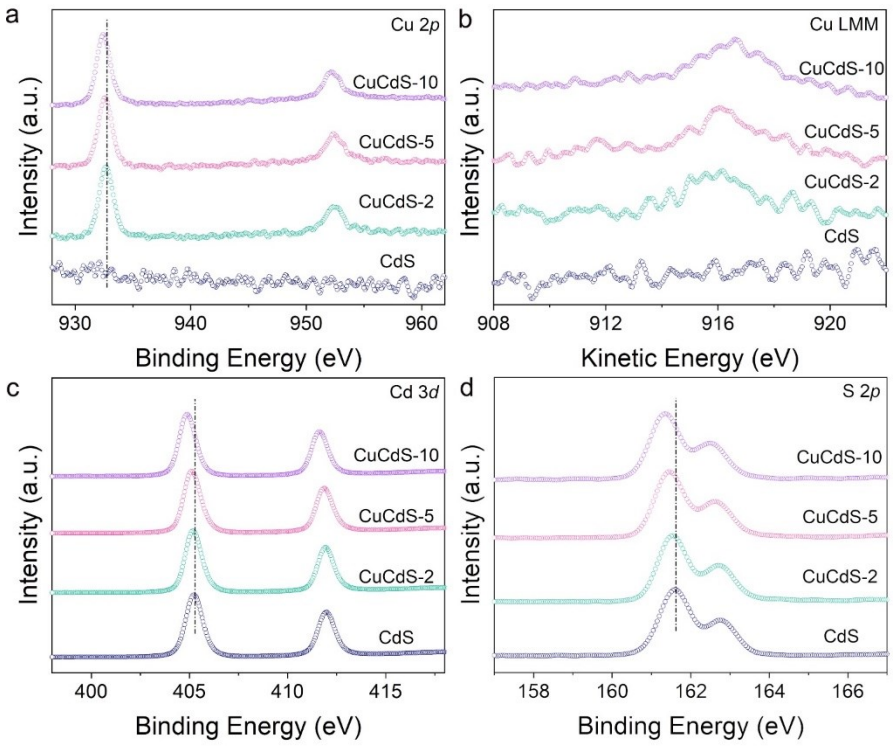

Fig. S6 High-resolution XPS spectra of (a) Cu 2p, (c) Cd 3d, (d) S 2p, and (b) Cu LMM Auger spectra for CdS, CuCdS-2, CuCdS-5 and CuCdS-10 photocatalysts.

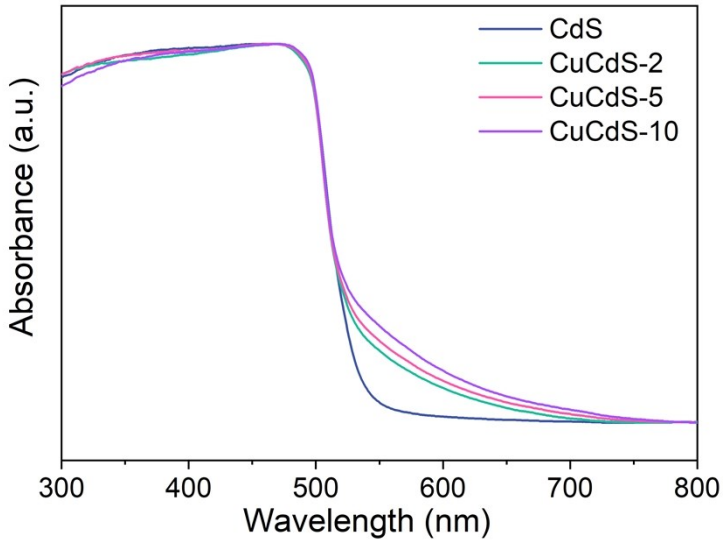

Fig. S7 UV-vis diffuse reflectance spectra of CdS, CuCdS-2, CuCdS-5 and CuCdS-10 photocatalysts.

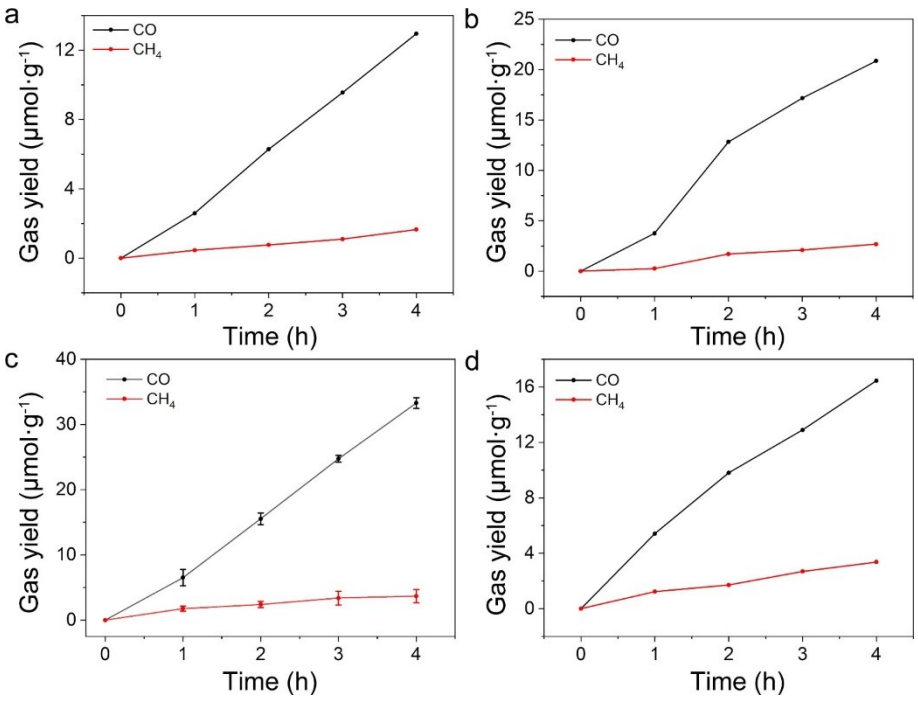

Fig. S8 The time course plots of CO and CH_4 evolution over (a) CdS, (b) CuCdS-2, (c) CuCdS-5 and (d) CuCdS-10 photocatalysts.

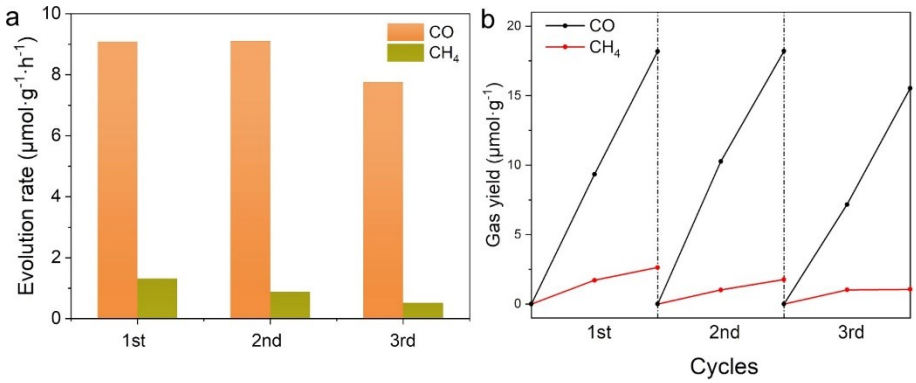

Fig. S9 Recycling experiments over CuCdS-5 during every 2 h of reaction time.

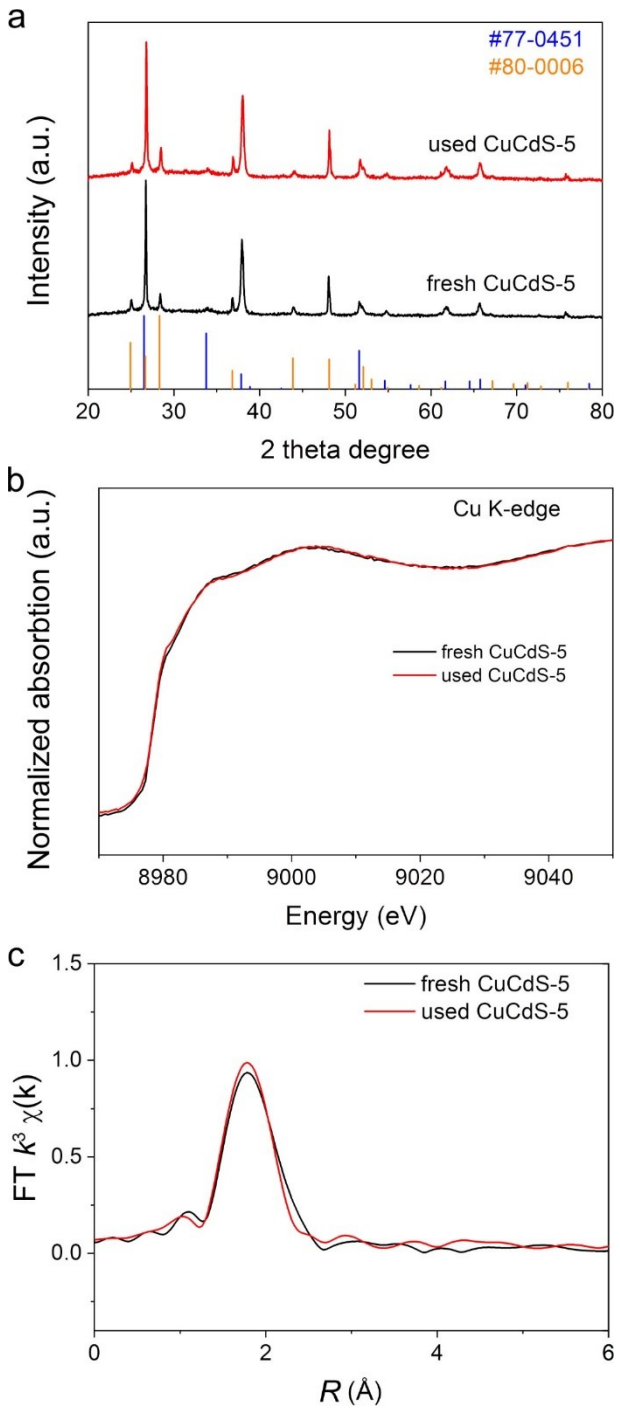

Fig. S10 Characterizations of fresh and used CuCdS-5. (a)The XRD patterns, (b)Cu *K*-edge NEXAFS spectra, (c) Fourier transformed k^3-weighted χ(k)-function of the Cu *K*-edge EXAFS spectra.

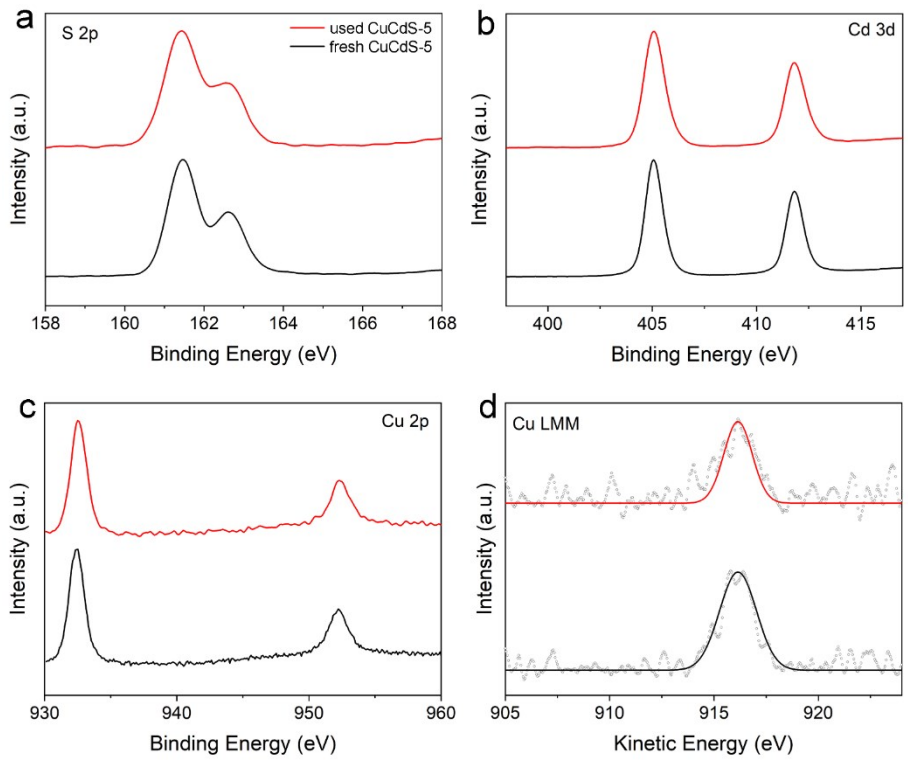

Fig. S11 High-resolution XPS spectra of (a) S 2p, (b) Cd 3d, (c) Cu 2p, and (d) Cu LMM Auger spectra for fresh and used CuCdS-5 photocatalyst.

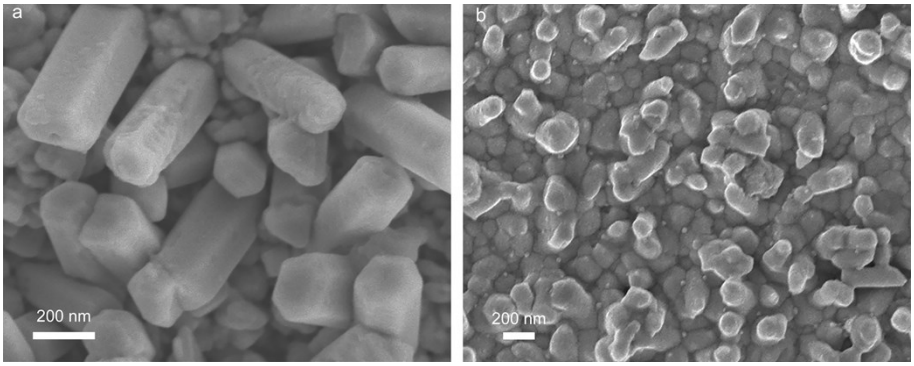

Fig. S12 SEM images of (a) CuCdS-10 and (b)CuCdS-300.

The surface of some CuCdS-10 nanorods became rougher in compared with that of CuCdS-5 and the pristine CdS without cation exchange, indicating the slight structural decomposition was happened on CuCdS-10 surface. When we further prolonged the cation exchange reaction time to 300 s, it can hardly maintain the nanorods morphology of CdS and the surface structure had been destroyed seriously.

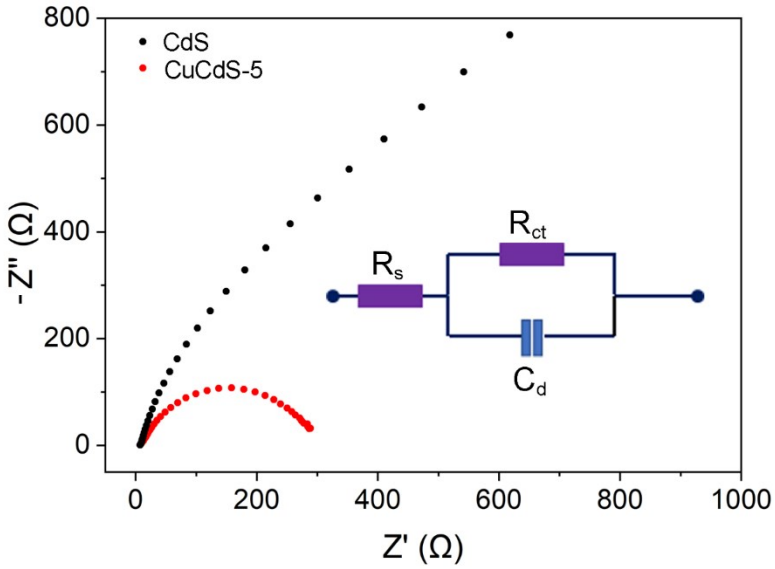

Fig. S13 Electrochemical impedance spectroscopy of CdS and CuCdS-5. (inset: Equivalent circuit diagram)

The anion vacancies have been demonstrated to promote interfacial charge transfer because of their abundant localized electrons and act as active sites for catalytic reactions, resulting in improved photocatalytic performance.[7,8] EIS tests for different samples were performed to identify the charge transfer and separation efficiency. The semi-circle at high frequency in the EIS Nyquist diagrams is equivalent to the charge transfer resistance across the electrode and electrolyte.[9] The CuCdS-5 shows better electronic conductivity indicated by a smaller semi-circle diameter than CdS, which suggests that the induced Cu sites and S vacancies efficiently improved the charge transfer.

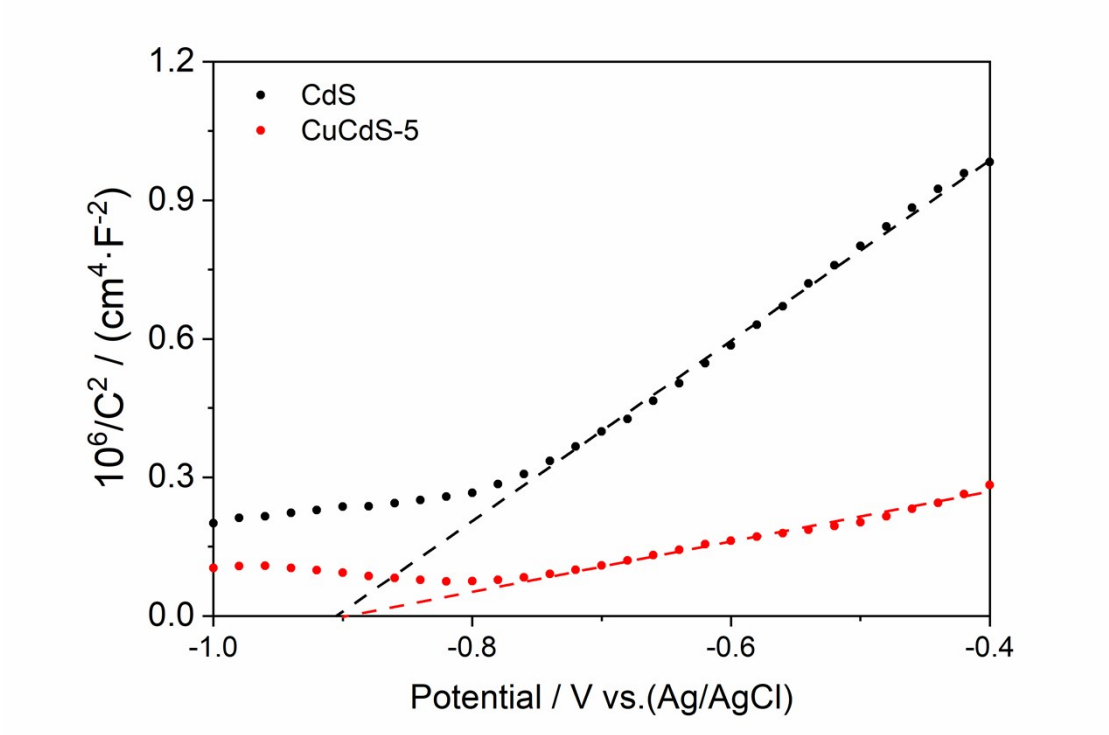

Fig. S14 Mott-Schottky plots of CdS and CuCdS-5 electrodes.

The carrier concentration can be calculated by the Mott-Schottky equation, where N_d, e, ε, ε_0, C and V_s represent the donor density, the electron charge, the dielectric constant, the permittivity of vacuum, space charge capacitance in the semiconductor and applied potential for MS measurement, respectively. It is assumed that the values of e, ε, ε_0 keep the same for CdS and CuCdS-5. Therefore, the CdS present a four-fold higher value of $1/C^2$ demonstrates the one-fourth (1/4) value of electron density of CdS to that of CuCdS-5 under the same bias potential.[10] A high electron density will lead to better electric conductivity and promote the charge transfer.

$$N_d = \frac{2}{e\varepsilon_0\varepsilon} \times \left[\frac{d\left(\frac{1}{C^2}\right)}{dV_s}\right] \quad (1)$$

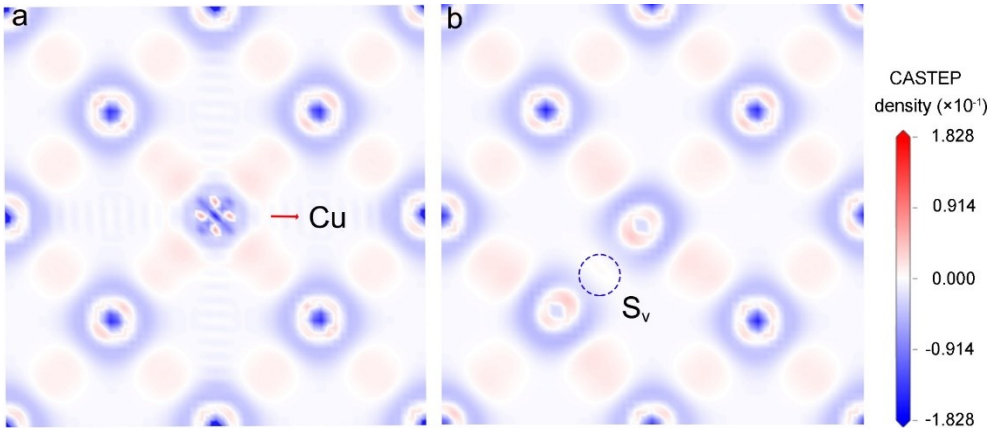

Fig. S15 Charge density difference diagrams of (a) Cu-CdS and (b) S_v-CdS. The red and blue color represents the charge accumulation and depletion, respectively.

The charge density difference analysis (as shown in Fig. 3b，3c and Fig.S15) clearly suggests that introducing Cu only, no additional electron transfer between Cu and S can be observed compared with the electron transfer between Cd and S (Fig.S5a vs. Fig. 3b). While introducing S vacancy only, one can observe a clear electron transfer from S vacancy to Cd (Fig. S15b vs. Fig. 3b). For simultaneously introducing Cu and S vacancy, similar electron transfer from S vacancy to Cu is further promoted (Fig. 3c vs. Fig. 3b).

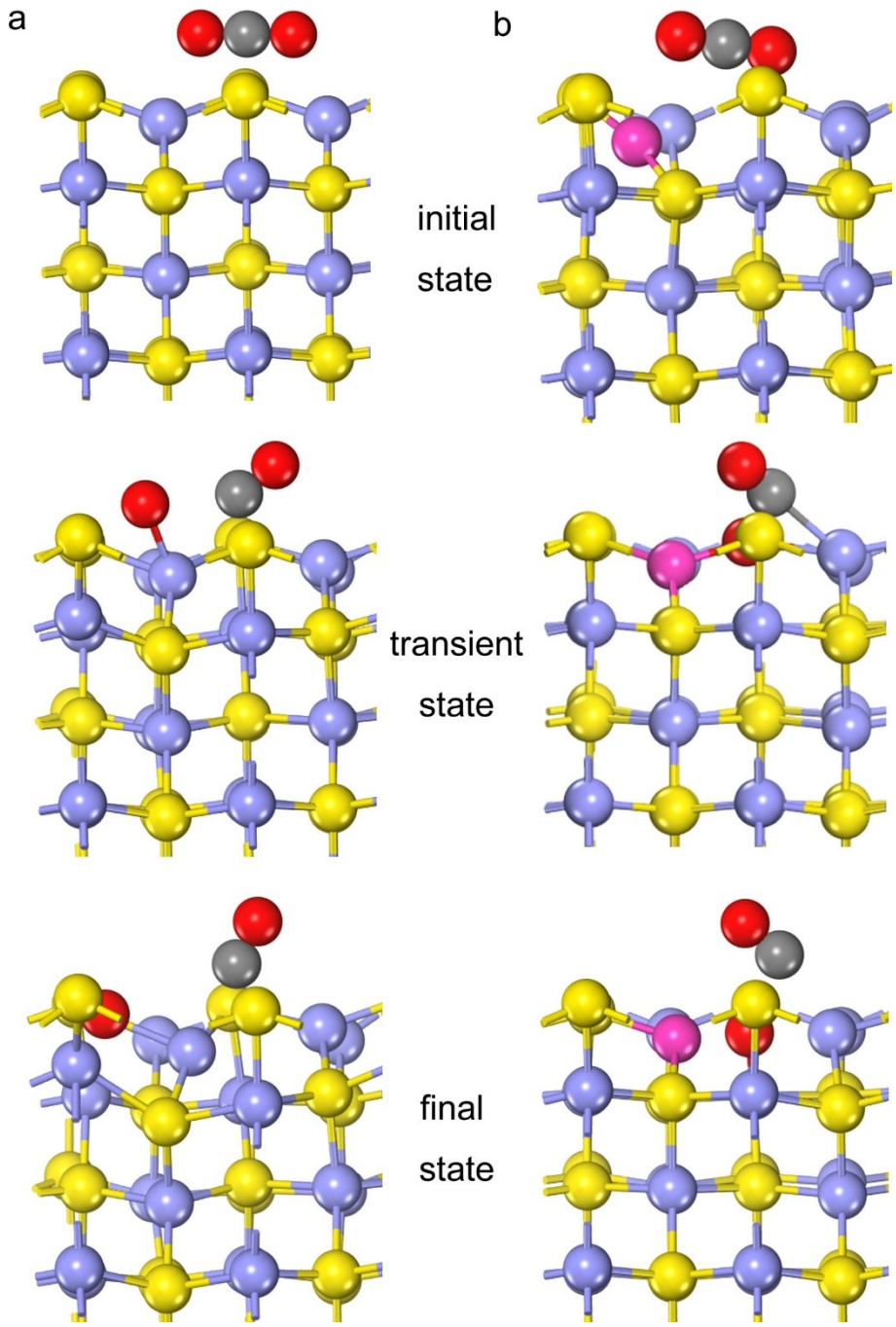

Fig. S16 Side views of the optimized structures of (a) CdS (b) CuCdS-5 in initial state, in transient state and in finally state during the progress of CO_2 dissociative adsorption. The Cd, S, Cu, C and O atoms are shown as the blue, yellow, purple, grey and red balls, respectively.

Table S1 The Cu/Cd atomic ratio quantified by ICP and XPS.

Sample	Cu/Cd atomic ratio (ICP)	Cu/Cd atomic ratio (XPS)
CdS	0	0
CuCdS-2	0.91%	4.68%
CuCdS-5	4.30%	8.46%
CuCdS-10	7.13%	13.42%

XPS spectra reveals that the Cu/Cd atomic ratio on the surface of CuCdS-5 is about 8.46%, which is far higher than that in ICP-OES results (4.30%), further demonstrating Cu species exist on the surface of CdS.

Table S2 Fit parameters obtained from the analysis of Cu *K*-edge EXAFS spectra.

Sample	path	CN	R (Å)	$\sigma^2(10^{-3}Å^2)$	ΔE_0 (eV)	R-factor
CuCdS-5	Cu-S	1.98	2.256	4.1	6.05	0.007

The first coordination number of the central atom Cu is about 2, suggesting that the proposed local structure is Cu-S2 in the surface region of CuCdS-5 which was demonstrated in Fig. 1i.

References

[1]. T. Ouyang, W. Fan, J. Guo, Y. Zheng, X. Yin and Y. Shen. *Phys. Chem. Chem. Phys*. 2020, **22**, 10305-10313.

[2]. J. Zhao, J. Zhao, F. Li and Z. Chen, *J. Phys. Chem. C*. 2018, **122**, 19712-19721.

[3]. X. An, S. Li, A. Yoshida, Z. Wang, X. Hao, A. Abudula and G. Guan, *ACS Sustain. Chem. Eng*. 2019, **7**, 9360-9368.

[4]. N. Kumari, N. Sinha, M. Haider and S. Basu, *Electrochim. Acta*, 2015, **177**,21-29.

[5]. J. Ren, H. Guo, J. Yang, Z. Qin, J. Lin and Z. Li, *Appl. Surf. Sci*. 2015, **351**, 504-516.

[6]. Q. Meng, T. Wang, E. Liu, X. Ma and Q. Ge. *Phys. Chem. Chem. Phys*. 2013, **15**, 9549-9563.

[7]. Q. Wu and R. Krol, *J. Am. Chem. Soc.*,2012, **134**, 9369-9375.

[8]. H. Li, J. Li, Z. Ai, F. Jia and L. Zhang, *Angew. Chem. Int. Edit.*, 2018, **57**, 122-138.

[9]. M. Takeno, T. Fukutsuka, K. Miyazaki and T. Abe, *J. Electrochem. Soc.*, 2017, **164**, A3862.

[10]. M. Xiao, L. Zhang, B. Luo, M. Lyu, Z. Wang, H. Huang, S. Wang, A. Du and L. Wang, *Angew. Chem. Int. Edit.* 2020, **132**, 7297-7301.